The *Drosophila melanogaster* enzyme glycerol-3-phosphate dehydrogenase 1 is required for oogenesis, embryonic development, and amino acid homeostasis

Madhulika Rai[1], Sarah M. Carter[1], Shefali A. Shefali[1], Nader H. Mahmoudzadeh[1], Robert Pepin[2], and Jason M. Tennessen[1§]

[1]Department of Biology, Indiana University, Bloomington, IN 47405, USA

[2] Department of Chemistry, Indiana University, Bloomington, IN, 47405, USA

[§] Correspondence: jtenness@indiana.edu

Keywords: *Drosophila*, metabolomics, glycerol-3-phosphate dehydrogenase, amino acid metabolism

ABSTRACT

As the fruit fly, *Drosophila melanogaster*, progresses from one life stage to the next, many of the enzymes that compose intermediary metabolism undergo substantial changes in both expression and activity. These predictable shifts in metabolic flux allow the fly meet stage-specific requirements for energy production and biosynthesis. In this regard, the enzyme Glyerol-3-phosphate dehydrogenase (GPDH1) has been the focus of biochemical genetics studies for several decades, and as a result, is one of the most well characterized *Drosophila* enzymes. Among the findings of these earlier studies is that GPDH1 acts throughout the fly lifecycle to promote mitochondrial energy production and triglyceride accumulation while also serving a key role in maintaining redox balance. Here we expand upon the known roles of GPDH1 during fly development by examining how depletion of both the maternal and zygotic pools of this enzyme influences development, metabolism, and viability. Our findings not only confirm previous observations that *Gpdh1* mutants exhibit defects in larval development, lifespan, and fat storage but also reveal that GPDH1 serves essential roles in oogenesis and embryogenesis. Moreover, metabolomics analysis reveals that a *Gpdh1* mutant stock maintained in a homozygous state exhibits larval metabolic defects that significantly differ from those observed in the F1 mutant generation. Overall, our findings highlight unappreciated roles for GPDH1 in early development and uncover previously undescribed metabolic adaptations that could allow flies to survive loss of this key enzyme.

39 **INTRODUCTION**

40 The *Drosophila* enzyme GPDH1 (encoded by FBgn0001128) is an ideal model for
41 understanding how metabolism adapts to the biosynthetic and energetic requirements of animal
42 development. Although the reaction catalyzed by GPDH1 is relatively simple (Figure 1), the
43 activity and purpose of the enzyme varies significantly during development. For example, GPDH1
44 is highly expressed in both the larval fat body and adult flight muscle but has opposite functions
45 within the two tissues. The larval fat body displays high levels of GPDH1 activity and relies on
46 this enzyme to generate glycerol-3-phosphate (G3P; Figure 1), which is used in triglyceride
47 synthesis (TAG) (RECHSTEINER 1970; SULLIVAN *et al.* 1983; MERRITT *et al.* 2006; LI *et al.* 2019).
48 Meanwhile, GPDH1 in adult flight muscle functions in conjunction with the mitochondrial enzyme
49 GPO1 to shuttle electrons into the electron transport chain for ATP synthesis (SACKTOR AND DICK
50 1962; O'BRIEN AND MACINTYRE 1972b; O'BRIEN AND MACINTYRE 1972a; WOJTAS *et al.* 1997;
51 MERRITT *et al.* 2006), thus supporting the intense energy demands of insect flight (Figure 1).

52 The distinct functions of GPDH1 within the larval fat body and adult flight muscles
53 illustrate why this enzyme serves as a model for understanding how metabolism is coordinately
54 regulated in the context of animal growth, development, and physiology. Nearly fifty years of
55 intensive biochemical and genetic studies revealed that GPDH1 kinetics, stability, and physical
56 characteristics vary dramatically between the larval and adult enzyme pool and that GPDH1
57 activity fluctuates as a function of developmental time, with activity levels peaking in L3 larvae
58 and in adults (WRIGHT AND SHAW 1969; RECHSTEINER 1970; O'BRIEN AND MACINTYRE 1972a;
59 SULLIVAN *et al.* 1983). These biochemical studies, coupled with decades of genetic analysis
60 (O'BRIEN AND MACINTYRE 1972b; O'BRIEN AND SHIMADA 1974; BEWLEY *et al.* 1980; KOTARSKI
61 *et al.* 1983; BURKHART *et al.* 1984; DAVIS AND MACINTYRE 1988; GIBSON *et al.* 1991;

62 YAMAGUCHI *et al.* 1994; MERRITT *et al.* 2006; CARMON *et al.* 2010; LI *et al.* 2019), make GPDH1
63 among the most intensively studied enzymes in developmental biology and provide insight
64 towards how normal animal development relies on dramatic changes in enzyme activity.

65 Despite *Gpdh1* serving as the subject of dozens of biochemical genetic studies, one pool
66 of GPDH1 remains largely overlooked. *Drosophila* embryos contain a significant amount of
67 maternally-loaded GPDH1 that potentially persists into larval development (WRIGHT AND SHAW
68 1969; WRIGHT AND SHAW 1970; CASAS-VILA *et al.* 2017). Yet, nearly all *Gpdh1* mutant studies
69 only examine zygotic mutants, raising the possibility that novel GPDH1 functions could be
70 discovered by examining mutants lacking the maternal enzyme pool. Here we address this
71 possibility by examining the metabolic and developmental defects displayed by maternal-zygotic
72 (M/Z) *Gpdh1* mutants. Our analysis reveals GPDH1 is not only required for normal oocyte
73 development but also that loss of the maternal GPDH1 pool leads to a significant embryonic lethal
74 phenotype. In contrast, among those *Gpdh1 M/Z* mutants that survive the embryonic lethal phase,
75 post-embryonic development and adult longevity appears similar between zygotic and M/Z *Gpdh1*
76 mutants. During our studies, however, we made the unexpected discovery that the homozygous
77 *Gpdh1* mutant stock used to study loss of the maternal GPDH1 enzyme pools exhibited striking
78 differences in the steady state levels of amino acids and tricarboxylic acid (TCA) metabolites when
79 compared with the control strain and F1 mutant generation. These unexpected findings provide
80 insight towards understanding how *Drosophila* metabolism is rewired to support the complete loss
81 of a major enzyme involved in central carbon metabolism.

82 **METHODS**

83 ***Drosophila melanogaster* husbandry and genetics**

84 Fly stocks were maintained on Bloomington *Drosophila* Stock Center (BDSC) food at 25ºC. The
85 $Gpdh1^{A10}$ mutant strain was described in a previous study from our lab (LI *et al.* 2019). For all the
86 experiments, 50 adult virgins were mated with 25 males and the embryos were collected on
87 molasses agar plates with yeast paste for 4 hours, as previously described (LI AND TENNESSEN
88 2017). $Gpdh1^{A10}$ zygotic mutant larvae were collected by crossing $Gpdh1^{A10}$*/CyO,*
89 *P{w[+mC]=GAL4-twi.G}2.2, P{w[+mC]=UAS-2xEGFP}AH2.2* males and females and selecting
90 for larvae lacking GFP expression. The *Gpdh1* maternal-zygotic mutant stock was established by
91 crossing $Gdph1^{A10}$ zygotic mutant males and females.

92

93 **Ovaries dissection and imaging**

94 Ovaries were dissected from $Gpdh1^{A10/+}$, $Gpdh1^{A10}$ *(Z) and* $Gpdh1^{A10}$ *(M/Z)* females that were
95 raised on yeast. Ovaries were fixed with 4% formaldehyde, rinsed twice with phosphate buffer
96 saline (PBS, pH 7.4), stained with DAPI for 30 minutes, and mounted on slides using vector shield
97 with DAPI (Vector Laboratories; H-1200-10). Slides were imaged using a Leica SP8 confocal
98 microscope.

99

100 **Fecundity analysis**

101 Twenty virgin females from $Gpdh1^{A10/+}$ (control), $Gpdh1^{A10}$ (Z) and $Gpdh1^{A10}$ (M/Z) were mated
102 with ten w^{1118} males in a small mating chamber. The total number of eggs laid during a two-hour
103 period was quantified for each mating chamber.

104

105 **Viability assays**

106 Embryonic viability of *Gpdh1*$^{A10/+}$, *Gpdh1*^{A10} *(Z)*, and *Gpdh1*^{A10} *(M/Z)* genotypes were
107 conducted by crossing 50 female virgins with 25 males in an egg-laying bottle that contained a
108 molasses agar plate partially covered with yeast paste (see LI AND TENNESSEN 2017). The egg-
109 laying plate was replaced every 24 hours for two days, after which time a fresh egg-laying plate
110 was placed in the bottle and eggs were collected for two hours. The egg-laying plate was removed,
111 and following an 8 hour incubation at 25ºC to allow for onset of GFP expression from the balancer
112 chromosomes, thirty non-GFP embryos were identified by circling the surrounding agar with a
113 dissecting needle. The number of eggs that hatched to become L1 larvae was recorded 24 hours
114 later.

115 Larval viability was measured by placing 20 synchronized embryos of each genotype on
116 molasses agar plates with yeast paste and measuring time until pupariation. Pupae were
117 subsequently transferred into a glass vial containing BDSC food and monitored until eclosion.

118

119 **Longevity assay**

120 Virgin female and male adults of the indicated genotypes were separated into glass vials (n = 10
121 adults/vial) and maintained at 25ºC. Flies were transferred to fresh vials every 5 days without the
122 use of carbon dioxide. The number of dead adults in each vial was recorded daily.

123

124 **Fat body staining**

125 Mid-L2 larval fat bodies were fixed and stained as previously described (TENNESSEN *et al.* 2014a).
126 Briefly, fat bodies were fixed with 4% formaldehyde, rinsed twice with PBS, once with 50%
127 ethanol, and then stained for 2 minutes at room temperature using filtered 0.5% Solvent Black 3

128 (CAS Number 4197-25-5; Sigma 199664) dissolved in 75% ethanol. Samples were sequentially
129 rinsed with 50% ethanol, 25% ethanol, and PBS. Stained tissues were mounted on a microscope
130 slide with vector shield with DAPI (Vector Laboratories; H-1200-10).
131

132 **Gas Chromatography-Mass Spectrometry (GC-MS) analysis**

133 GC-MS analysis was performed at the Indiana University Mass Spectrometry Facility as
134 previously described (LI AND TENNESSEN 2018). All samples contained 25 mid-L2 larvae and six
135 biological replicates were analyzed per genotype. GC-MS data was normalized based on sample
136 mass and an internal succinic-d4 acid standard that was present within the extraction buffer. Data
137 were analyzed using Metaboanalyst version 5.0 following log transformation (base 10) and Pareto
138 Scaling (PANG *et al.* 2021).
139

140 **Adult body mass measurements**

141 Ten adult male or female flies were collected one day post-eclosion, placed into pre-tared 1.5 mL
142 microfuge tubes, and the mass was measured using a Mettler XS 105 weighing analytical balance.
143 Six independent samples were measured per genotype.
144

145 **Statistical Analysis**

146 Unless noted, statistical analysis was conducted using GraphPad Prism v9.1. Data are presented as
147 scatter plots, with error bars representing the standard deviation and the line in the middle
148 representing the mean value. Unless noted, data was compared using a Kruskal-Wallis test
149 followed by a Dunn's multiple comparison test. Longevity data was analyzed using a log-rank
150 (Mantel-Cox) test.

151

152 **RESULTS AND DISCUSSION**

153 **GPDH1 is required for oogenesis and embryonic viability**

154 Previous studies indicate that GPDH1 is expressed in the ovary and maternally loaded into
155 the egg (WRIGHT AND SHAW 1969; WRIGHT AND SHAW 1970; CASAS-VILA *et al.* 2017).
156 Considering that homozygous *Gpdh1* mutant strains are reported to be sub-viable (O'BRIEN AND
157 MACINTYRE 1972b; O'BRIEN AND SHIMADA 1974; KOTARSKI *et al.* 1983; MERRITT *et al.* 2006),
158 we examined the possibility that GPDH1 serves essential roles during early development that have
159 been previously overlooked. As a first step towards testing this possibility, we dissected the ovaries
160 from the homozygous $Gpdh1^{A10}$ mutant flies – both from F1 mutants (generated by crossing
161 $Gpdh1^{A10}$*/CyO, twi-GFP* parents and selecting for GFP^{-} larvae), as well as from a homozygous
162 $Gpdh1^{A10}$ mutant strain (designated *M/Z* to indicate a complete absence of enzyme during
163 development). We found that the ovaries from both F1 $Gpdh1^{A10}$ females and $Gpdh1^{A10}$ *M/Z*
164 females were smaller than those observed in control females and contained fewer late-stage
165 ovarioles (Figure 2A-C). Notably, we regularly observed degenerating egg chambers in mutant
166 embryos (See Figure 2B, arrow), indicating that loss of GPDH1 in females limits oocyte
167 production. Consistent with the observed egg chamber defects, both classes of *Gpdh1* mutants
168 exhibit significant decreases in egg-laying as compared with controls (Figure 2D).

169 As a complement to our studies of oogenesis, we also examined if the maternal and zygotic
170 GPDH1 enzyme pools are required for embryonic development. Females of a control strain
171 ($Gpdh1^{A10/+}$), F1 *Gpdh1* mutants ($Gpdh1^{A10}$) and the *Gpdh1* mutant strain ($Gpdh1^{A10}$ *M/Z)* were
172 crossed with either w^{1118} controls or $Gpdh1^{A10}$ mutant males and the resulting offspring were
173 scored for the percentage of embryos that hatched to first instar larvae (L1). We observed that
174 embryos from *Gpdh1* mutant mothers of either genetic background died at a significantly higher

175 rate than those produced by heterozygous control mothers, regardless of the parental genotype
176 (Figure 2E), indicating that both the maternal and zygotic GPDH1 pools are required during
177 embryogenesis. Overall, our findings that *Gpdh1* mutants display oogenesis defects and embryonic
178 lethality explains why *Gpdh1* mutant females exhibit such low levels of fecundity when compared
179 with control strains.
180
181 **Zygotic and Maternal-Zygotic *Gpdh1* mutants display similar defects during larval**
182 **development and adult longevity**
183 The observed requirement for maternal GPDH1 in embryogenesis led us to reevaluate if
184 loss of this enzyme pool also influences development and lifespan in later life stages. Like previous
185 reports of *Gpdh1* zygotic mutants, we found the *Gpdh1 M/Z* mutant larvae develop more slowly
186 than heterozygous controls and ~20% fail to initiate metamorphosis (Figure 3A). These
187 developmental delay phenotypes, however, are indistinguishable from *Gpdh1* zygotic mutants
188 (Figure 3A). Moreover, *Gpdh1 M/Z* mutants eclose at the same rate as zygotic mutants (Figure
189 3B). The only observable difference between the zygotic and *M/Z* mutants is that newly eclosed
190 *Gpdh1 M/Z* mutants females exhibit slightly increased body mass (Figure 3C), however, we are
191 unable to rule out the possibility that this phenotype is due to differences in genetic background.
192 As a complement to our studies of larval development, we also examine the viability of
193 *Gpdh1* mutant adults. Here too, we observe little difference between F1 *Gpdh1* mutants and *M/Z*
194 mutants. Consistent with earlier findings (MERRITT *et al.* 2006), we observed that both the
195 $Gpdh1^{A10}$ zygotic mutant females and *M/Z* mutant females are short-lived when compared with a
196 heterozygous controls strain, with a majority mutant animals dying within two weeks of eclosion
197 (Figure 4A). However, we observed that the short lifespan phenotype was milder in F1 $Gpdh1^{A10}$

198 mutant males and absent in the *Gpdh1*^{A10} *M/Z* mutant males (Figure 4B). The observed decrease
199 in female *Gpdh1* lifespan is apparent while maintaining the maternal-zygotic stock on
200 Bloomington *Drosophila* Stock Center food. Although bottles of the *Gpdh1*^{A10} *M/Z* mutant strain
201 contains approximately equal ratios of males:females two days after eclosion, this ratio becomes
202 significantly skewed two weeks post-eclosion due to females dying earlier than male mutants
203 (Figure 4C). Overall, our findings reveal that nearly all growth, development, and viability
204 phenotypes exhibited by the *Gpdh1*^{A10} *M/Z* mutants are no more severe than those observed in the
205 F1 *Gpdh1*^{A10} mutants.
206

207 ***Gpdh1* zygotic mutants and maternal-zygotic mutants exhibit significant differences in**
208 **amino acid metabolism**

209 Larval development is able to compensate for loss of zygotic GPDH1 by inducing
210 compensatory changes in central carbon metabolism, rendering *Gpdh1* mutants dependent on LDH
211 and GPO1 activity while also inducing significant changes in redox balance and steady-state amino
212 acid levels (DAVIS AND MACINTYRE 1988; LI *et al.* 2019). These earlier metabolic studies were
213 conducted by crossing males and females from a heterozygous *Gpdh1*$^{-}$*/CyO,twi-GFP* stock and
214 selecting for homozygous offspring, thus providing a readout of how loss of zygotic GPDH1
215 affects larval metabolism. In this regard, our homozygous *Gpdh1 M/Z* mutant strain provides a
216 unique opportunity to determine if loss of both the maternal and zygotic enzyme pools induce a
217 distinct metabolic profile when compared with zygotic mutants. Towards this goal, we first
218 examined larval triglyceride (TAG) levels in the heterozygous control, F1 *Gpdh1* mutant, and the
219 homozygous *Gpdh1 M/Z* strain. Consistent with previous studies (MERRITT *et al.* 2006), we
220 observed similar decreases in fat body TAG levels of the *Gpdh1*^{A10} zygotic and *Gpdh1*^{A10} *M/Z*

221 mutant larvae when compared with *Gpdh1*$^{A10/+}$ heterozygous controls (Figure 5A-C). These results
222 indicate that loss of the maternal GPDH1 pool does not exacerbate the *Gpdh1* TAG mutant
223 phenotype.

224 We next used a targeted GC-MS-based approach to compare the levels of amino acids,
225 TCA cycle intermediates, and glycolytic end products in mid-L2 larvae of *Gpdh1*$^{A10/+}$
226 heterozygous controls, *Gpdh1*^{A10} zygotic mutants, and *Gpdh1*^{A10} *M/Z* mutants (Table S1). When
227 the resulting metabolomics data was analyzed using principal component analysis, the *Gpdh1*^{A10}
228 *M/Z* mutant samples clearly separated from both the *Gpdh1*^{A10} zygotic mutants and the *Gpdh1*$^{A10/+}$
229 heterozygous controls (Figure 6A), suggesting that the three genotypes have distinct metabolic
230 profiles. A closer analysis of the datasets revealed that the changes observed in *Gpdh1*^{A10} zygotic
231 mutant larvae mimic those observed previously (Li *et al.* 2019) – G3P levels were significantly
232 decreased in relative to the control strain (Figure 6B,C) and both lactate and 2-hydroxyglutarate
233 remained at comparable levels (Figure 6B, D, E). The relative abundance of some amino acids and
234 TCA cycle intermediates were also decreased in the zygotic *Gpdh1* mutant larvae compared with
235 *Gpdh1*$^{A10/+}$ controls (Figure 6B,F,G,H).

236 While the metabolite changes observed in *Gpdh1* zygotic mutants largely confirmed
237 previous studies, the metabolic profile of the *Gpdh1*^{A10} *M/Z* mutants exhibited striking differences.
238 Even though G3P, lactate, and 2-hydroxyglutare levels were comparable between the two mutant
239 genotypes (Figure 6B-E), many of the same amino acids that were either decreased or unchanged
240 in the zygotic mutants were significantly elevated in the *M/Z* mutant background (Figure 6B, F-
241 H). For example, relative to the control strain, tyrosine and β-alanine were decreased by 40% and
242 30%, respectively, in zygotic mutants but increased by 40% and 25% in the maternal-zygotic
243 mutant (Figure 6G,H). A similar trend was observed with the TCA intermediates succinate,

244 fumarate, and malate (Figure 6B), with the relative abundance of malate exhibiting a ~15%
245 decrease in zygotic mutants and a 25% increase in maternal-zygotic mutants when compared to
246 the heterozygous control strain. The results are notable because they support a previously
247 published hypothesis that *Gpdh1* mutants experience compensatory changes in malate metabolism
248 (MERRITT *et al.* 2006). Overall, our results reveal that a strain lacking both the maternal and zygotic
249 GPDH1 enzyme pool exhibit changes in the steady-state levels of amino acid and TCA cycle
250 intermediates that are opposite of those observed in mutants lacking only the zygotic enzyme
251 contribution. Future studies should determine if these changes are due to either genetic selection
252 when establishing the homozygous *Gpdh1* mutant stock or directly result from loss of the maternal
253 GPDH1 enzyme pool.
254
255

256 **DISCUSSION**

257 Here we demonstrate the *Drosophila* enzyme GPDH1 serves essential roles in both
258 oogenesis and embryogenesis. Our findings expand the known roles for GPDH1 and raise
259 questions as to what function this enzyme serves during early development. Considering that the
260 purpose of GPDH1 activity differs in a context specific manner (*e.g.*, TAG synthesis in fat body,
261 ATP production in flight muscle), our findings raise the question as to the function of GPDH1 in
262 these developmental contexts. Moreover, G3P levels are known to increase over the course of
263 embryogenesis (TENNESSEN *et al.* 2014b), suggesting that this compound serves a unique role in
264 the developing embryo.

265 Our findings also demonstrate that larvae lacking both maternal and zygotic GPDH1
266 activity exhibit developmental phenotypes that are largely indistinguishable from *Gpdh1* zygotic
267 mutants. However, targeted metabolomics analysis indicates that *Gpdh1 M/Z* mutants exhibit
268 metabolic phenotypes that are more severe than the zygotic mutants, raising the question as to how
269 loss of maternal enzyme pool can influence the larval metabolic program in such a dramatic
270 manner. While we can't rule out the possibility that maternal GPDH1 activity establishes a
271 metabolic state in the embryo that persists into larval development, a more likely explanation stems
272 from the fact that oogenesis and embryogenesis are energetic processes that impose intense
273 demands on cellular metabolism. As a result, generation of the homozygous *Gpdh1* mutant strain
274 would inevitably select for background mutations that compensate for loss of GPDH1 activity in
275 the ovary and embryos – a hypothesis that is supported by previous observations. For example,
276 even though GPDH1 is essential for maintaining ATP production in flight muscle (O'BRIEN AND
277 MACINTYRE 1972b; WOJTAS *et al.* 1997; MERRITT *et al.* 2006), *Gpdh1* mutants slowly regain the
278 ability to fly when maintained in lab culture (O'BRIEN AND SHIMADA 1974), indicating that other

279 metabolic processes must be able to compensate for loss of GPDH1 activity. Similarly, *Gpdh1*
280 larvae only exhibit slight developmental delays despite displaying a significant disruption in redox
281 balance. This ability of larvae to maintain a somewhat normal growth rate in the absence of
282 GPDH1 depends on the enzymes LDH and GPO1, as loss of either enzyme in a *Gpdh1* mutant
283 background enhances the mutant phenotype (DAVIS AND MACINTYRE 1988; LI *et al.* 2019). These
284 earlier studies, combined with our findings and previous observations that *Gpdh1* phenotypes are
285 highly dependent on genetic background (MERRITT *et al.* 2006), indicate that GPDH1 functions
286 within a complex and highly adaptable metabolic network that warrants further study.

287 Regardless of the reason for why *Gpdh1* maternal-zygotic mutants exhibit significant
288 metabolic differences when compared with zygotic mutants, our study highlights a poorly
289 understood relationship between G3P and amino acid metabolism. While we are unsure as to the
290 significance of this metabolic relationship in the fly, our findings are consistent with studies of a
291 mouse model of GPD1 deficiency, which induces compensatory amino acid metabolism during
292 fasting in mice (SATO *et al.* 2016). One intriguing possibility is that the *Gpdh1* maternal-zygotic
293 mutants induce changes in one of the central metabolic regulating pathways that control amino
294 acid metabolism. In this regard, the amino acid sensor Tor is not only known to regulate the yeast
295 glycerol-3-phosphate dehydrogenase 1 activity in yeast (LEE *et al.* 2012), but the GPDH1
296 substrate, DHAP (see Figure 1), but also activates Tor in mammalian cell culture (OROZCO *et al.*
297 2020). These correlations between Gpdh1 and Tor should be the subject of future investigations.

298 Our studies also revealed changes in the relative abundance of a subset of TCA acid cycle
299 intermediates. These observations suggest that mitochondrial metabolism in *Gpdh1* maternal-
300 zygotic mutants is fundamentally altered when compared with controls and zygotic mutants.
301 Considering that GPDH1 is an essential enzyme in the G3P shuttle, which shuttles electrons to the

302 mitochondria for ATP production (Figure 1), the observed increases in succinate, fumarate, and
303 malate hint at the possibility that maternal-zygotic mutants exhibit significant changes in
304 mitochondrial metabolism. However, since we observe no changes in the relative abundance of
305 alanine, lactate, and 2-hydroxyglutarate, which are commonly elevated in flies that experience
306 disruption of mitochondrial activity (FEALA *et al.* 2007; COQUIN *et al.* 2008; CAMPBELL *et al.*
307 2019; MAHMOUDZADEH *et al.* 2020), the significance of these changes in *Gpdh1* maternal-zygotic
308 mutant remain unclear.

309 Overall, our results again emphasize that GPDH1 serves a unique role in *Drosophila*
310 metabolism. The studies presented herein both confirms a large body of literature regarding the
311 role of GPDH1 in physiology, development, and lifespan and reveals new roles for this enzyme in
312 oogenesis, embryogenesis, and amino acid metabolism. Moreover, considering that several studies
313 hint at a key role for human GPD1 in cancer metabolism (ZHOU *et al.* 2017; RUSU *et al.* 2019; LIU
314 *et al.* 2021; XIA *et al.* 2021), our findings highlight the need to better understand how this highly
315 studied enzyme influences gene expression, cell growth and differentiation, and metabolic
316 signaling networks.
317

318 **ACKNOWLEDGMENTS**

319 We thank the Bloomington *Drosophila* Stock Center (NIH P40OD018537) for providing fly
320 stocks, the *Drosophila* Genomics Resource Center (NIH 2P40OD010949) for genomic reagents,
321 and Flybase (NIH 5U41HG000739) and the Indiana University Light Microscopy Imaging Center.
322 Targeted GC-MS analysis was conducted using instruments housed in the Indiana University Mass
323 Spectrometry Facility, which is supported, in part, by NSF MRI Award 1726633. J.M.T. is
324 supported by the National Institute of General Medical Sciences of the National Institutes of Health
325 under a R35 Maximizing Investigators' Research Award (MIRA; 1R35GM119557).

326

327 **FIGURE LEGENDS**

328 **Figure 1. GPDH1 promotes cytosolic redox balance, ATP production, and TAG**
329 **accumulation.** A schematic diagram illustrating the role of GPDH1 in central carbon metabolism.
330 GPDH1 relies on the cofactor NAD^+/NADH to interconvert the glycolytic intermediate
331 dihydroxyacetone phosphate (DHAP) to glycerol 3-phosphate (G3P). In *Drosophila* larvae, the
332 GPDH1-dependent conversion of DHAP to G3P functions in parallel with Lactate Dehydrogenase
333 (LDH) to maintain redox balance. G3P is used as a precursor for TAG synthesis and functions in
334 the G3P electron shuttle to transfer reducing equivalents to the electron transport chain. In adult
335 flight muscle, GPDH1 function in conjunction with GPO1 and the tricarboxylic acid (TCA) cycle
336 to generate the ATP required for flight. Abbreviations: dihydroxyacetone phosphate (DHAP),
337 glyceraldehyde-3-phosphate (GA3P), glycerol-3-phosphate (G3P), glycerol-3-phosphate
338 dehydrogenase (GPDH1), glycerophosphate oxidase 1 (GPO1), lactate dehydrogenase (LDH),
339 mitochondrial pyruvate carrier 1 (MPC1), pyruvate dehydrogenase (PDH), tricarboxylic acid
340 (TCA).

341

342 **Figure 2. *Gpdh1* is required for oocyte development and embryonic viability.** (A-C) Ovaries
343 were dissected from 3-day old females and stained with DAPI. When compare to the $Gpdh1^{A10/+}$
344 control strain (A), the ovaries of (B) F1 generation $Gpdh1^{A10}$ mutants and (C) $Gpdh1^{A10}$ *M/Z*
345 mutants display (B,C) fewer later stage oocytes and (B) degenerating egg chambers (see arrow).
346 (D) The fecundity of F1 generation $Gpdh1^{A10}$ mutants and $Gpdh1^{A10}$ *M/Z* mutants are significantly
347 decreased when compared with controls. (E) Embryos produced by either F1 generation $Gpdh1^{A10}$
348 mutants or $Gpdh1^{A10}$ *M/Z* mutants exhibit significant mortality when compared with the controls

349 and independent of paternal genotype. *P< 0.05. **P< 0.01. ***P< 0.001. P-values calculated
350 using a Kruskal-Wallis tests followed by a Dunn's test.
351
352 **Figure 3. *Gpdh1* zygotic and *Gpdh1* maternal-zygotic mutants exhibit similar developmental**
353 **delays.** *Gpdh1*$^{A10/+}$ controls, F1 generation *Gpdh1*^{A10} mutants, and *Gpdh1*^{A10} *M/Z* mutants were
354 analyzed for (A) time from egg-laying to pupariation, (B) time from egg-laying to eclosion, and
355 (C) body mass one day after eclosion. For (B), the % eclosion value represents the percent of pupae
356 that successfully eclosed and does not include the 20% of larvae that failed to pupariate. **P<
357 0.01. P-values calculated using a Kruskal-Wallis tests followed by a Dunn's test.
358
359 **Figure 4. *Gpdh1* mutant females are short-lived.** The lifespan of (A) females and (B) males
360 from *Gpdh1*$^{A10/+}$ heterozygous controls, F1 generation *Gpdh1*^{A10} mutants, and a *Gpdh1*^{A10} *M/Z*
361 mutant strain were analyzed for 80 days after eclosion. Longevity data was analyzed using a log-
362 rank (Mantel-Cox) test. (C) Ratio of males to females in culture bottles either 2 or 14 days after
363 eclosion. *P< 0.05. P-values calculated using an unpaired t-test.
364
365 **Figure 5. TAG levels are significantly decreased in *Gphd1* mutants.** Representative images of
366 mid-L2 fat bodies stained with Black Solvent 2 and imaged using bright field microscopy. When
367 compared with (A) heterozygous *Gpdh1*$^{A10/+}$ control, both (B) F1 generation *Gpdh1*^{A10} mutants
368 (C) a *Gpdh1*^{A10} *M/Z* mutant strain exhibit a similar decrease in lipid levels.
369
370 **Figure 6. Metabolomic analysis of *Gpdh1* zygotic and *Gpdh1* maternal-zygotic mutants.**

371 A targeted GC-MS-based metabolomics method was used to compare the relative abundance of
372 G3P, lactate, 2HG and amino acids, between heterozygous *Gpdh1*$^{A10/+}$ controls, *Gpdh1*^{A10}
373 zygotic mutants and *Gpdh1*^{A10} maternal-zygotic mutants. (A) PCA plot showing that the control,
374 F1 generation *Gpdh1* mutants *(Z)*, and the *Gpdh1 M/Z* mutant strain separate clearly in their
375 metabolomic profile. (B) Heatmap showing the increase in the relative abundance of amino acids
376 in *Gpdh1 M/Z* mutants when compared to the F1 generation *Gpdh1* zygotic mutants and the
377 *Gpdh1*$^{A10/+}$ controls. (C-H) The relative abundance of (C) G3P, (D) lactate, and (E) 2HG, (F)
378 malate, (G) tyrosine, and (H) b-alanine are represented as scatter plots with the horizontal lines
379 representing the mean value and standard deviation. *P< 0.05. **P< 0.01. ***P< 0.001. P-
380 values calculated using a Kruskal-Wallis tests followed by a Dunn's test. Analysis in (A) and (B)
381 conducted using MetaboAnalyst 5.0 (see methods).
382
383 **SUPPLEMENTAL TABLES**
384 **Table S1. GC-MS analysis of control, *Gpdh1* zygotic mutants, and *Gpdh1* maternal-zygotic**
385 **mutants.** Samples contained 25 mid-L2 larvae. Data normalized to sample mass and a d4-
386 succinic acid internal standard.
387

LITERATURE CITED

Bewley, G. C., J. M. DeZurik and G. Pagelson, 1980 Analysis of l-glycerol-3-phosphate dehydrogenase mutants in *Drosophila melanogaster*: complementation for intracellular degradation of the mutant polypeptide. Mol Gen Genet 178**:** 301-308.

Burkhart, B. D., E. Montgomery, C. H. Langley and R. A. Voelker, 1984 Characterization of Allozyme Null and Low Activity Alleles from Two Natural Populations of *DROSOPHILA MELANOGASTER*. Genetics 107**:** 295-306.

Campbell, J. B., S. Werkhoven and J. F. Harrison, 2019 Metabolomics of anoxia tolerance in *Drosophila melanogaster*: evidence against substrate limitation and for roles of protective metabolites and paralytic hypometabolism. Am J Physiol Regul Integr Comp Physiol 317**:** R442-R450.

Carmon, A., J. Chien, D. Sullivan and R. MacIntyre, 2010 The alpha glycerophosphate cycle in *Drosophila melanogaster* V. molecular analysis of alpha glycerophosphate dehydrogenase and alpha glycerophosphate oxidase mutants. J Hered 101**:** 218-224.

Casas-Vila, N., A. Bluhm, S. Sayols, N. Dinges, M. Dejung *et al.*, 2017 The developmental proteome of *Drosophila melanogaster*. Genome Res 27**:** 1273-1285.

Coquin, L., J. D. Feala, A. D. McCulloch and G. Paternostro, 2008 Metabolomic and flux-balance analysis of age-related decline of hypoxia tolerance in *Drosophila* muscle tissue. Mol Syst Biol 4**:** 233.

Davis, M. B., and R. J. MacIntyre, 1988 A genetic analysis of the alpha-glycerophosphate oxidase locus in *Drosophila melanogaster*. Genetics 120**:** 755-766.

Feala, J. D., L. Coquin, A. D. McCulloch and G. Paternostro, 2007 Flexibility in energy metabolism supports hypoxia tolerance in *Drosophila* flight muscle: metabolomic and computational systems analysis. Mol Syst Biol 3**:** 99.

Gibson, J. B., A. Cao, J. Symonds and D. Reed, 1991 Low activity sn-glycerol-3-phosphate dehydrogenase variants in natural populations of *Drosophila melanogaster*. Heredity (Edinb) 66 (Pt 1)**:** 75-82.

Kotarski, M. A., S. Pickert, D. A. Leonard, G. J. LaRosa and R. J. MacIntyre, 1983 The characterization of alpha-glycerophosphate dehydrogenase mutants in *Drosophila melanogaster*. Genetics 105**:** 387-407.

Lee, Y. J., G. R. Jeschke, F. M. Roelants, J. Thorner and B. E. Turk, 2012 Reciprocal phosphorylation of yeast glycerol-3-phosphate dehydrogenases in adaptation to distinct types of stress. Mol Cell Biol 32**:** 4705-4717.

Li, H., M. Rai, K. Buddika, M. C. Sterrett, A. Luhur *et al.*, 2019 Lactate dehydrogenase and glycerol-3-phosphate dehydrogenase cooperatively regulate growth and carbohydrate metabolism during *Drosophila melanogaster* larval development. Development 146.

Li, H., and J. M. Tennessen, 2017 Methods for studying the metabolic basis of *Drosophila* development. Wiley Interdiscip Rev Dev Biol 6.

Li, H., and J. M. Tennessen, 2018 Preparation of *Drosophila* Larval Samples for Gas Chromatography-Mass Spectrometry (GC-MS)-based Metabolomics. J Vis Exp.

Liu, R., Y. Feng, Y. Deng, Z. Zou, J. Ye *et al.*, 2021 A HIF1alpha-GPD1 feedforward loop inhibits the progression of renal clear cell carcinoma via mitochondrial function and lipid metabolism. J Exp Clin Cancer Res 40**:** 188.

Mahmoudzadeh, N. H., A. J. Fitt, D. B. Schwab, W. E. Martenis, L. M. Nease *et al.*, 2020 The oncometabolite L-2-hydroxyglutarate is a common product of dipteran larval development. Insect Biochem Mol Biol 127**:** 103493.

Merritt, T. J., E. Sezgin, C. T. Zhu and W. F. Eanes, 2006 Triglyceride pools, flight and activity variation at the *Gpdh* locus in *Drosophila melanogaster*. Genetics 172**:** 293-304.

O'Brien, S. J., and R. J. MacIntyre, 1972a The -glycerophosphate cycle in *Drosophila melanogaster*. I. Biochemical and developmental aspects. Biochem Genet 7**:** 141-161.

436 O'Brien, S. J., and R. J. Macintyre, 1972b The -glycerophosphate in *Drosophila melanogaster*. II. Genetic
437 aspects. Genetics 71**:** 127-138.
438 O'Brien, S. J., and Y. Shimada, 1974 The alpha-glycerophosphate cycle in *Drosophila melanogaster*. IV.
439 Metabolic, ultrastructural, and adaptive consequences of alphaGpdh-l "null" mutations. J Cell Biol
440 63**:** 864-882.
441 Orozco, J. M., P. A. Krawczyk, S. M. Scaria, A. L. Cangelosi, S. H. Chan *et al.*, 2020 Dihydroxyacetone
442 phosphate signals glucose availability to mTORC1. Nat Metab 2**:** 893-901.
443 Pang, Z., J. Chong, G. Zhou, D. A. de Lima Morais, L. Chang *et al.*, 2021 MetaboAnalyst 5.0: narrowing
444 the gap between raw spectra and functional insights. Nucleic Acids Res 49**:** W388-W396.
445 Rechsteiner, M. C., 1970 *Drosophila* lactate dehydrogenase and alpha-glycerolphosphate dehydrogenase:
446 distribution and change in activity during development. J Insect Physiol 16**:** 1179-1192.
447 Rusu, P., C. Shao, A. Neuerburg, A. A. Acikgoz, Y. Wu *et al.*, 2019 GPD1 Specifically Marks Dormant
448 Glioma Stem Cells with a Distinct Metabolic Profile. Cell Stem Cell 25**:** 241-257 e248.
449 Sacktor, B., and A. Dick, 1962 Pathways of hydrogen transport in the oxidation of extramitochondrial
450 reduced diphosphopyridine nucleotide in flight muscle. J Biol Chem 237**:** 3259-3263.
451 Sato, T., Y. Yoshida, A. Morita, N. Mori and S. Miura, 2016 Glycerol-3-phosphate dehydrogenase 1
452 deficiency induces compensatory amino acid metabolism during fasting in mice. Metabolism 65**:**
453 1646-1656.
454 Sullivan, D. T., F. A. Donovan and G. Skuse, 1983 Developmental regulation of glycerol-3-phosphate
455 dehydrogenase synthesis in *Drosophila*. Biochem Genet 21**:** 49-62.
456 Tennessen, J. M., W. E. Barry, J. Cox and C. S. Thummel, 2014a Methods for studying metabolism in
457 *Drosophila*. Methods 68**:** 105-115.
458 Tennessen, J. M., N. M. Bertagnolli, J. Evans, M. H. Sieber, J. Cox *et al.*, 2014b Coordinated metabolic
459 transitions during *Drosophila* embryogenesis and the onset of aerobic glycolysis. G3 (Bethesda) 4**:**
460 839-850.
461 Wojtas, K., N. Slepecky, L. von Kalm and D. Sullivan, 1997 Flight muscle function in *Drosophila* requires
462 colocalization of glycolytic enzymes. Mol Biol Cell 8**:** 1665-1675.
463 Wright, D. A., and C. R. Shaw, 1969 Genetics and ontogeny of alpha-glycerophosphate dehydrogenase
464 isozymes in *Drosophila melanogaster*. Biochem Genet 3**:** 343-353.
465 Wright, D. A., and C. R. Shaw, 1970 Time of expression of genes controlling specific enzymes in
466 *Drosophila* embryos. Biochem Genet 4**:** 385-394.
467 Xia, R., H. Tang, J. Shen, S. Xu, Y. Liang *et al.*, 2021 Prognostic value of a novel glycolysis-related gene
468 expression signature for gastrointestinal cancer in the Asian population. Cancer Cell Int 21**:** 154.
469 Yamaguchi, Y., T. S. Takano, T. Yamazaki and K. Harada, 1994 Molecular analysis of Gpdh null mutations
470 that arose in mutation accumulation experiments in *Drosophila melanogaster*. Heredity (Edinb) 73
471 (Pt 4)**:** 397-404.
472 Zhou, C., J. Yu, M. Wang, J. Yang, H. Xiong *et al.*, 2017 Identification of glycerol-3-phosphate
473 dehydrogenase 1 as a tumour suppressor in human breast cancer. Oncotarget 8**:** 101309-101324.

474

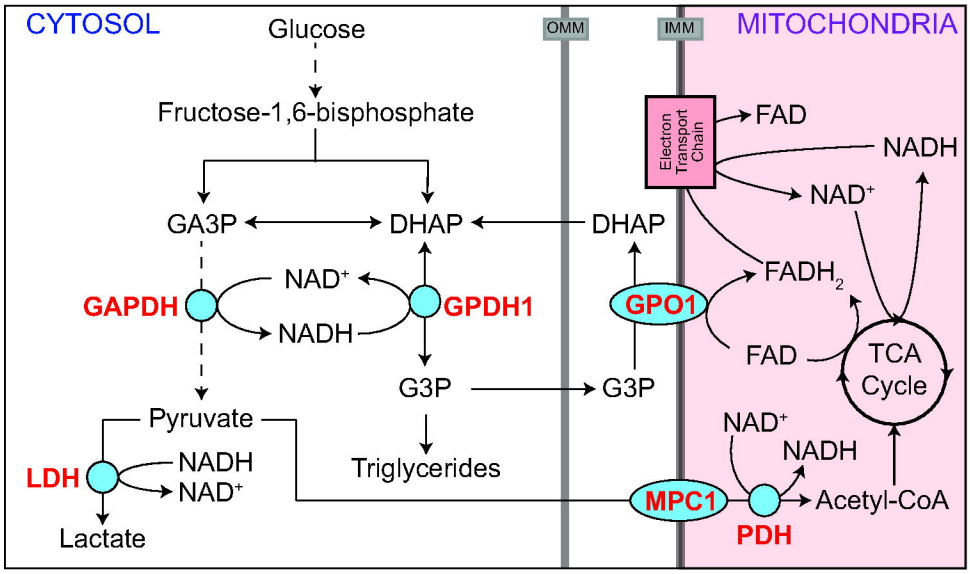

Figure 1. GPDH1 promotes cytosolic redox balance, ATP production, and TAG accumulation. A schematic diagram illustrating the role of GPDH1 in central carbon metabolism. GPDH1 relies on the cofactor NAD^+/NADH to interconvert the glycolytic intermediate dihydroxyacetone phosphate (DHAP) to glycerol 3-phosphate (G3P). In *Drosophila* larvae, the GPDH1-dependent conversion of DHAP to G3P functions in parallel with Lactate Dehydrogenase (LDH) to maintain redox balance. G3P is used as a precursor for TAG synthesis and functions in the G3P electron shuttle to transfer reducing equivalents to the electron transport chain. In adult flight muscle, GPDH1 function in conjunction with GPO1 and the tricarboxylic acid (TCA) cycle to generate the ATP required for flight. Abbreviations: dihydroxyacetone phosphate (DHAP), glyceraldehyde-3-phosphate (GA3P), glycerol-3-phosphate (G3P), glycerol-3-phosphate dehydrogenase (GPDH1), glycerophosphate oxidase 1 (GPO1), lactate dehydrogenase (LDH), mitochondrial pyruvate carrier 1 (MPC1), pyruvate dehydrogenase (PDH), tricarboxylic acid (TCA).

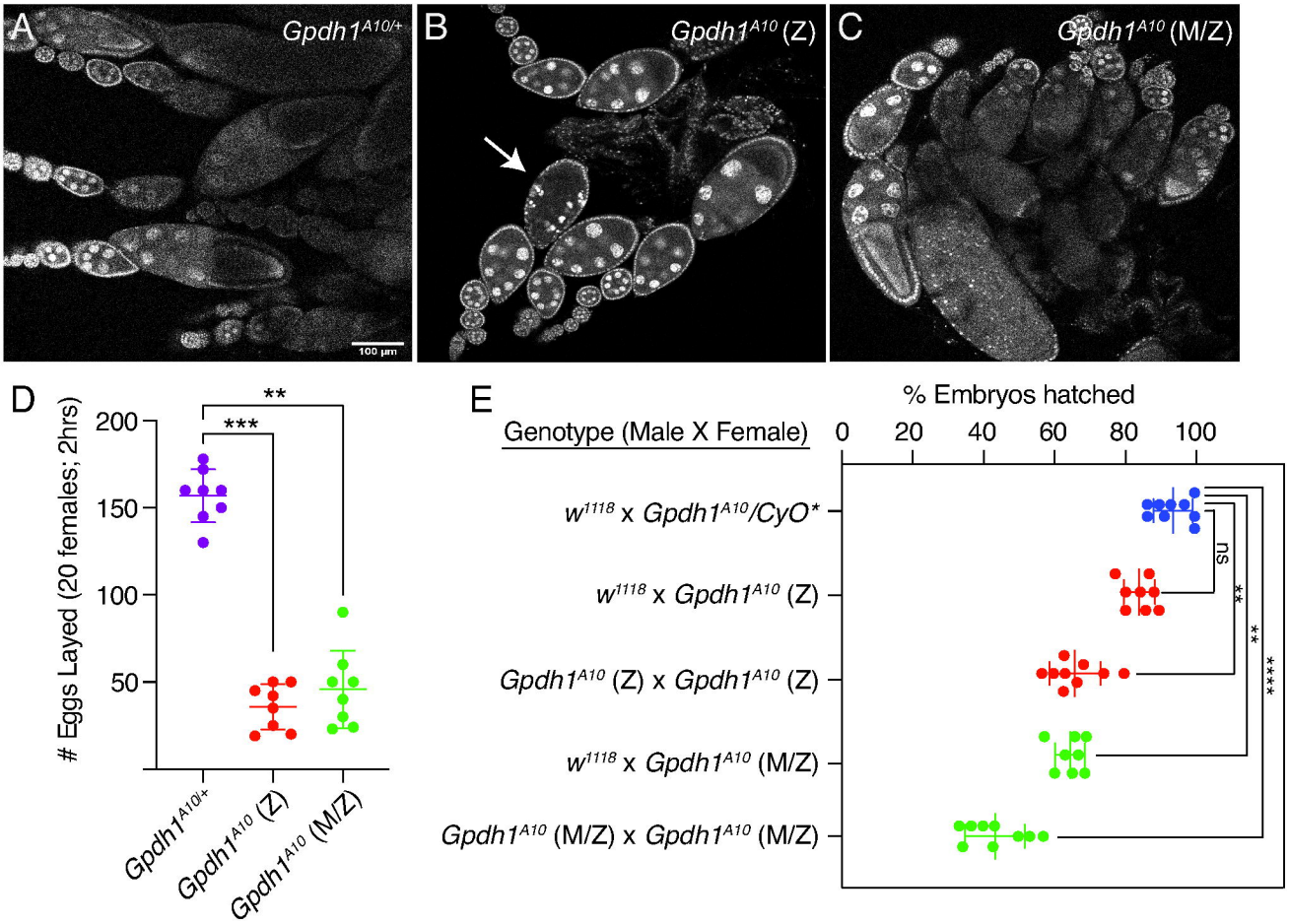

Figure 2. *Gpdh1* is required for oocyte development and embryonic viability. (A-C) Ovaries were dissected from 3-day old females and stained with DAPI. When compare to the *Gpdh1*$^{A10/+}$ control strain (A), the ovaries of (B) F1 generation *Gpdh1*^{A10} mutants and (C) *Gpdh1*^{A10} *M/Z* mutants display (B,C) fewer later stage oocytes and (B) degenerating egg chambers (see arrow). (D) The fecundity of F1 generation *Gpdh1*^{A10} mutants and *Gpdh1*^{A10} *M/Z* mutants are significantly decreased when compared with controls. (E) Embryos produced by either F1 generation *Gpdh1*^{A10} mutants or *Gpdh1*^{A10} *M/Z* mutants exhibit significant mortality when compared with the controls and independent of paternal genotype. *P< 0.05. **P< 0.01. ***P< 0.001. P-values calculated using a Kruskal-Wallis tests followed by a Dunn's test.

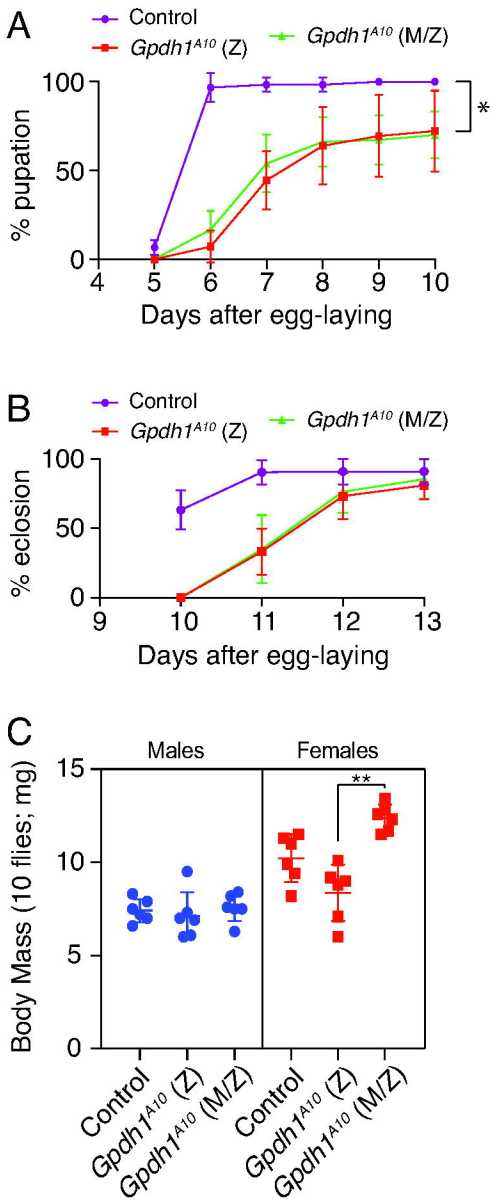

Figure 3. *Gpdh1* zygotic and *Gpdh1* maternal-zygotic mutants exhibit similar developmental delays. *Gpdh1*$^{A10/+}$ controls, F1 generation *Gpdh1*^{A10} mutants, and *Gpdh1*^{A10} *M/Z* mutants were analyzed for (A) time from egg-laying to pupariation, (B) time from egg-laying to eclosion, and (C) body mass one day after eclosion. For (B), the % eclosion value represents the percent of pupae that successfully eclosed and does not include the 20% of larvae that failed to pupariate. ***P*< 0.01. *P*-values calculated using a Kruskal-Wallis tests followed by a Dunn's test.

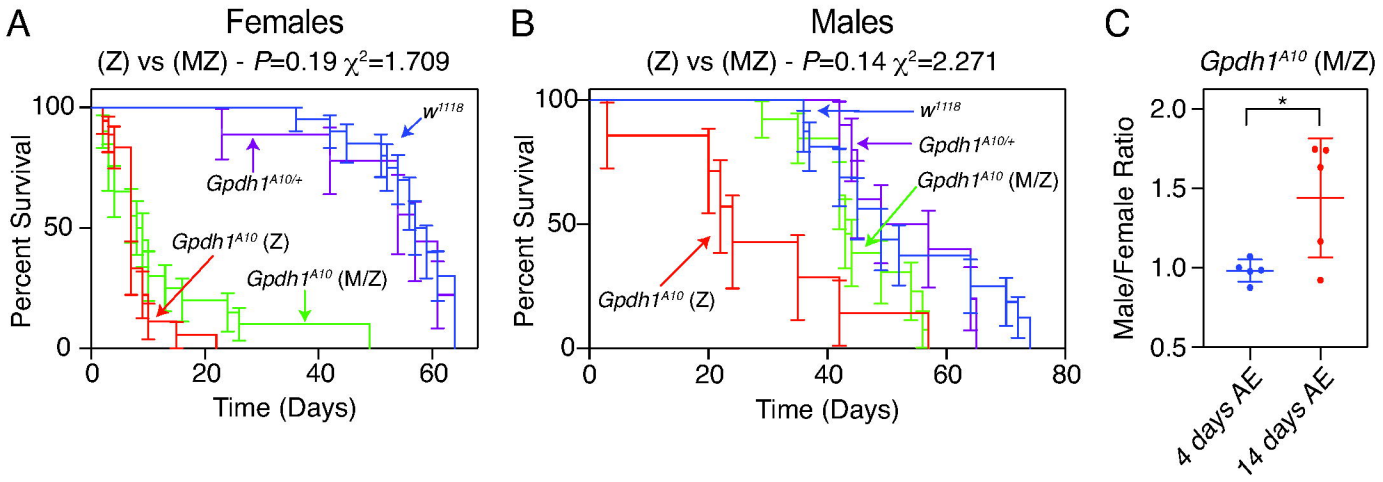

Figure 4. *Gpdh1* mutant females are short-lived. The lifespan of (A) females and (B) males from *Gpdh1*$^{A10/+}$ heterozygous controls, F1 generation *Gpdh1*^{A10} mutants, and a *Gpdh1*^{A10} *M/Z* mutant strain were analyzed for 80 days after eclosion. Longevity data was analyzed using a log-rank (Mantel-Cox) test. (C) Ratio of males to females in culture bottles either 2 or 14 days after eclosion. *$P < 0.05$. *P*-values calculated using an unpaired t-test.

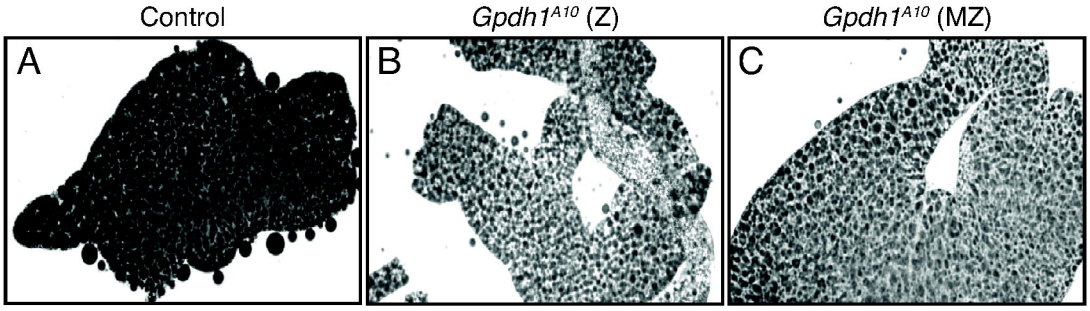

Figure 5. TAG levels are significantly decreased in *Gphd1* mutants. Representative images of mid-L2 fat bodies stained with Black Solvent 2 and imaged using bright field microscopy. When compared with (A) heterozygous *Gpdh1*$^{A10/+}$ control, both (B) F1 generation *Gpdh1*^{A10} mutants (C) a *Gpdh1*^{A10} *M/Z* mutant strain exhibit a similar decrease in lipid levels.

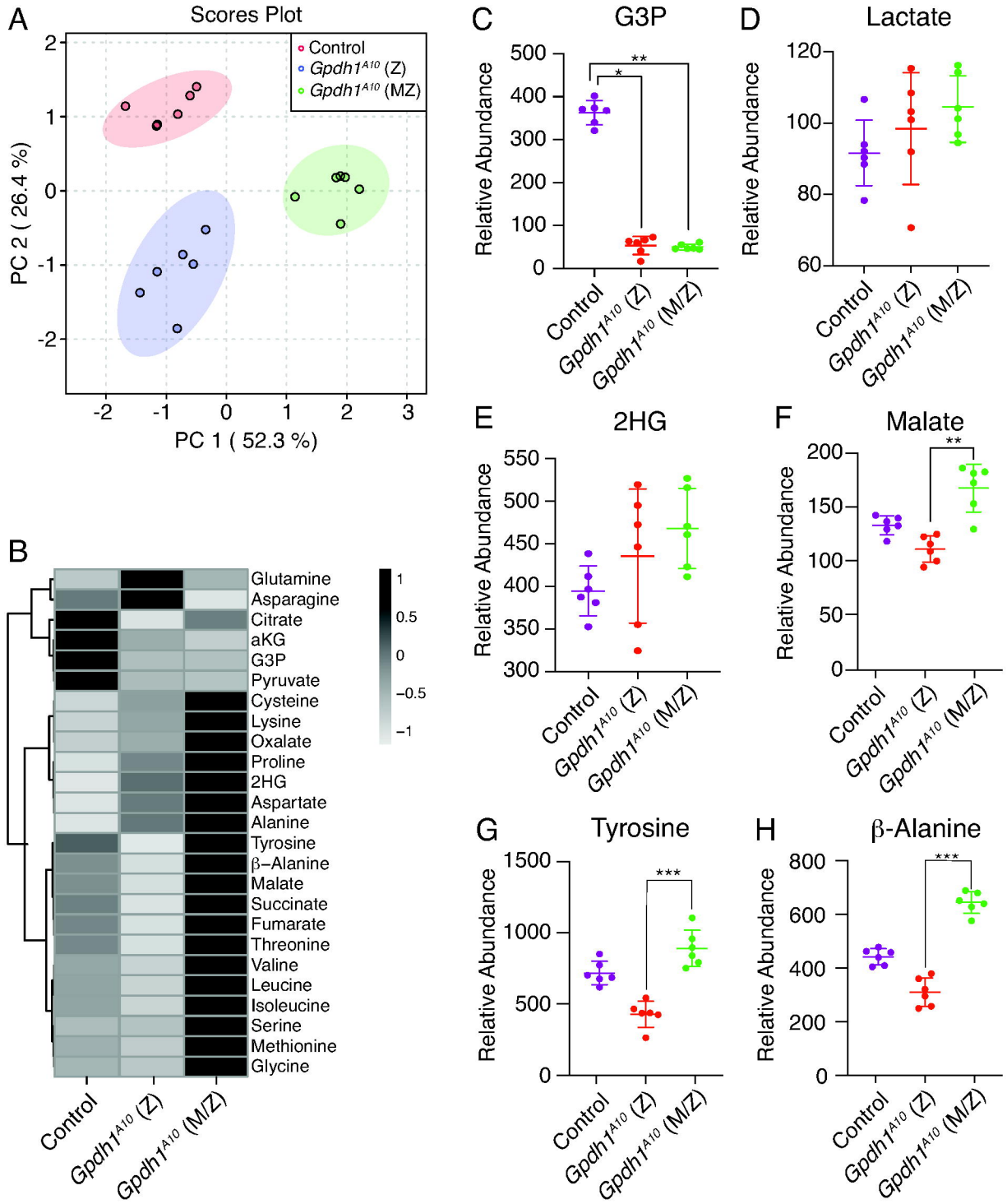

Figure 6. Metabolomic analysis of *Gpdh1* zygotic and *Gpdh1* maternal-zygotic mutants. A targeted GC-MS-based metabolomics method was used to compare the relative abundance of G3P, lactate, 2HG and amino acids, between heterozygous *Gpdh1*$^{A10/+}$ controls, *Gpdh1*^{A10} zygotic mutants and *Gpdh1*^{A10} maternal-zygotic mutants. (A) PCA plot showing that the control, F1 generation *Gpdh1* mutants *(Z)*, and the *Gpdh1 M/Z* mutant strain separate clearly in their metabolomic profile. (B) Heatmap showing the increase in the relative abundance of amino acids in *Gpdh1 M/Z* mutants when compared to the F1 generation *Gpdh1* zygotic mutants and the *Gpdh1*$^{A10/+}$ controls. (C-H) The relative abundance of (C) G3P, (D) lactate, and (E) 2HG, (F) malate, (G) tyrosine, and (H) β-alanine are represented as scatter plots with the horizontal lines representing the mean value and standard deviation. **P*< 0.05. ***P*< 0.01. ****P*< 0.001. *P*-values calculated using a Kruskal-Wallis tests followed by a Dunn's test. Analysis in (A) and (B) conducted using MetaboAnalyst 5.0 (see methods).